frontiers | Frontiers in Immunology

TYPE Original Research
PUBLISHED 10 January 2025
DOI 10.3389/fimmu.2024.1528721

OPEN ACCESS

EDITED BY
Patricia Pereiro,
Spanish National Research Council (CSIC), Spain

REVIEWED BY
Jianfei Lu,
Ningbo University, China
Fuguo Liu,
Massachusetts Institute of Technology, United States

*CORRESPONDENCE
Lucienne Garcia Pretto-Giordano
lgiordano@uel.br
Laurival Antônio Vilas-Boas
lavboas@uel.br
Jorge Manuel de Oliveira Fernandes
jorge.fernandes@icm.csic.es

RECEIVED 15 November 2024
ACCEPTED 23 December 2024
PUBLISHED 10 January 2025

CITATION
Appel RJC, Siqueira KN, Konstantinidis I, Martins MIM, Joshi R, Pretto-Giordano LG, Vilas-Boas LA and Fernandes JMdO (2025) Comparative transcriptome analysis reveals a serotype-specific immune response in Nile tilapia (*Oreochromis niloticus*) infected with *Streptococcus agalactiae*. *Front. Immunol.* 15:1528721. doi: 10.3389/fimmu.2024.1528721

Comparative transcriptome analysis reveals a serotype-specific immune response in Nile tilapia (*Oreochromis niloticus*) infected with *Streptococcus agalactiae*

Renan José Casarotto Appel[1,2], Karine Nicole Siqueira[2], Ioannis Konstantinidis[1], Maria Isabel Mello Martins[3], Rajesh Joshi[4], Lucienne Garcia Pretto-Giordano[5]*, Laurival Antônio Vilas-Boas[2]* and Jorge Manuel de Oliveira Fernandes[1,6]*

[1]Faculty of Biosciences and Aquaculture, Nord University, Bodø, Norway, [2]Department of General Biology, State University of Londrina, Londrina, Brazil, [3]Department of Veterinary Clinics, State University of Londrina, Londrina, Brazil, [4]GenoMar Genetics AS, Oslo, Norway, [5]Department of Preventive Veterinary Medicine, State University of Londrina, Londrina, Brazil, [6]Department of Renewable Marine Resources, Institute of Marine Sciences (ICM-CSIC), Barcelona, Spain

Streptococcus agalactiae is a major causative agent of streptococcosis in Nile tilapia (*Oreochromis niloticus*) and understanding its etiology is important to ensure the sustainable development of global tilapia farming. Our research group recently observed contrasting disease patterns in animals infected with two different *S. agalactiae* serotypes (Ib and III). To better understand the basis for these divergent responses, we analyzed the brain transcriptome of Nile tilapia following bacterial exposure. Our findings revealed significant variation in the expression of genes involved in immune (e.g., *CD209* antigen, *granulin*, C-X-C motif chemokine 10, prostacyclin synthase, and interleukins) and neuroendocrine (e.g., *mmp13a*, *mmp9*, *brain aromatase*, and *pmch*) pathways. The serotype Ib strain seems promptly recognized by the host, triggering a potent inflammatory response, whereas the serotype III strain elicited a less immediate response, resulting in more pronounced central nervous system (CNS) symptoms and behavioral effects. To the best of our knowledge, this is the first study to show serotype-specific immune responses to *S. agalactiae* in Nile tilapia. These findings are important for advancing disease management and control strategies in aquaculture. Identifying different immune reactions triggered by serotypes Ib and III may assist the development of more specific approaches for preventive measures, early detection, and effective treatment against streptococcosis.

KEYWORDS

Nile tilapia, brain, streptococcosis, immunity, aquaculture, gene expression, RNAseq

1 Introduction

The aquaculture industry is continuously evolving towards more intensive cultivation systems. Although this shift has led to a production increase, it has also promoted the proliferation of opportunistic and pathogenic bacteria (1). Tilapia farming has become one of the most important industries in the aquaculture sector (2), making Nile tilapia (*Oreochromis niloticus*) the second-most cultivated fish globally (1, 3). Rising consumer demand for high-quality animal protein has led to a diversification in the tilapia production systems, with the farms now ranging from conventional small-scale culture to intensive high-density stocking systems (4). However, this intensification resulted in a significant challenge: disease outbreaks. High stocking densities and consequent poor water quality create stressful conditions that suppress the fish immune system, making them more vulnerable to infections and facilitating disease transmission.

Among bacterial diseases in tilapia, streptococcosis causes significant economic losses for producers worldwide (5, 6). *Streptococcus agalactiae*, a Gram-positive encapsulated bacterium, is the main pathogen associated with streptococcosis (7–9). The disease manifests with severe clinical signs, such as loss of appetite, scoliosis, ascites, exophthalmia, corneal opacity, and meningoencephalitis, leading to neurological symptoms like disorientation and erratic swimming (10, 11). Current strategies to combat streptococcosis include vaccination, antibiotics, and selective breeding for genetic resistance (2, 12). However, the diversity of *S. agalactiae* serotypes makes disease control challenging, with isolates showing unique pathogenic profiles and treatment responses (13–16). *S. agalactiae* is classified into ten serotypes (Ia, Ib, II, III, IV, V, VI, VII, VIII, and IX) based on capsular antigens (17), with serotypes Ia, Ib, and III being the most common in fish worldwide (18).

Despite extensive research on the overall development of streptococcosis, including the effects of temperature (19–21) and diet (22–25) on disease progression, gene expression variance within fish (26–29), and pathogen immune evasion mechanisms (30–32), our understanding of the divergent infection symptoms and host immune responses to different bacterial serotypes remains limited.

Our research group recently isolated two different serotypes of *S. agalactiae* following streptococcosis outbreaks in Brazil: SA8-UEL (serotype Ib), isolated in Paraná state, and SA10-UEL (serotype III) from Maranhão. After further investigation, it was possible to notice different infection response patterns in Nile tilapia exposed to these strains, with the SA10-UEL strain inducing severe neurological symptoms, including erratic swimming and a high mortality rate in the initial days of infection. In contrast, the SA8-UEL strain exhibited slower disease progression with less pronounced brain-related symptoms (personal observations, unpublished).

Understanding how distinct serotype infections influence immune pathways, blood-brain barrier (BBB) integrity, and neuroendocrine functions is indispensable for predicting and managing streptococcosis dynamics. To address this knowledge gap, we conducted a transcriptome analysis to characterize the brain response in Nile tilapia following exposure to two *S. agalactiae* strains of different serotypes.

2 Materials and methods

2.1 Ethics statement

All experiments in this study were conducted in strict accordance with the guidelines established by the Animal Ethics Committee of the State University of Londrina, Brazil (process n° CEUA 45/2017).

2.2 Fish rearing

Male Nile tilapia (average weight 20 ± 2 g) were obtained from the Vivenda Flora Tropical fingerling fish farm at Londrina, Paraná, Brazil. The fish were acclimated in a 1000 L tank for 15 days and fed twice a day with extruded commercial feed (3% body weight) manufactured by Integrada Agricultural Cooperative, Brazil. Water temperature was kept at 28.0 ± 0.5°C using heating rods (model RS-300, RS Electrical), with a pH range of 6.8–7.2. Dissolved oxygen levels ranged from 7 to 8 ppm, and the photoperiod was maintained at a 14:10-h light:dark schedule.

2.3 *S. agalactiae* strains

The two strains of *S. agalactiae*, SA8-UEL (serotype Ib) (accession number SUB14593605) and SA10-UEL (serotype III) (accession number SUB14593588), were cultured in liquid tryptic soy broth (TSB) (Acumedia) at 30 °C overnight without agitation. The cultures were subcultured into 100 mL TSB broth following the same conditions for 8 h. Bacterial concentration was determined in colony-forming units (CFU) per mL by plating 10 µL of 10-fold serial dilutions on tryptic soy agar (TSA) (Acumedia) plates (33).

2.4 Fish challenge and sample collection

Prior to the experiment, we randomly selected 1% of the animals received for pre-screening. These fish were anesthetized and euthanized, and their kidneys were collected for plating on selective media and PCR analysis by amplification of the 16S rRNA gene using the F1 (5'-GAG TTT GAT CAT GGC TCA G-3') and Imod (5'-ACC AAC ATG TGT TAA TTA CTC-3') primers. Both tests confirmed that the animals were not infected with *S. agalactiae* before the formal challenge experiment. After a 24-hour fasting period, 260 Nile tilapia were randomly divided into three experimental groups: a control group of 20 fish, and two challenged groups with six replicate tanks containing 20 fish each for the SA8-UEL and SA10-UEL strains. Fish were housed in 50 L aquaria. Before bacterial inoculation, the fish were anesthetized with eugenol (100 mg/L) for 30-40 s and intraperitoneally injected with 0.1 mL/fish of bacterial suspension (8×10^7 CFU/mL for SA8-UEL, and 4×10^7 CFU/mL for SA10-UEL). In contrast, control group fish were injected with an equal volume of TSB broth (Acumedia). The bacterial concentrations were selected based on prior experiments

to identify minimum concentrations that induce neurological symptoms, such as erratic swimming, in approximately 20% of the animals challenged with *S. agalactiae*. After inoculation, the animals were maintained in a freshwater flow-through system following the same conditions as during the acclimation period.

After bacterial exposure, the fish were fed and monitored daily over the next 15 days for the development of clinical symptoms. The primary objective of the study was to evaluate gene expression in brain tissue after the appearance of erratic swimming behavior, a sign indicative of central nervous system (CNS) damage. Fish were examined daily and those exhibiting such clinical symptoms were promptly removed from the aquaria, euthanized by medullary section, and their brain was collected; a counterpart from the control group was also sampled, except for one SA8-UEL and SA10-UEL strains. The brain tissue was collected immediately after euthanasia by performing a cranial cut with a sterile scalpel and removing the brain using a sterile clamp. The brain was placed in cryogenic tubes containing 1.5 mL of RNAlater (Sigma-Aldrich) and immediately frozen in liquid nitrogen. All time points for sample collection are detailed in Supplementary Table 1.

2.5 RNA extraction, library construction, and sequencing

Frozen brain samples were homogenized in QIAzol lysis reagent (Qiagen) at 5,000 × g for 20 s with zirconium oxide beads (1.4 mm; Precellys) in a Precellys® 24 homogenizer (Bertin Instruments). RNA was extracted using Direct-zol™ RNA MiniPrep (Zymoresearch) following the manufacturer's instructions. RNA concentration, purity, and quality were assessed using NanoDrop™ 1,000 (Thermo Fisher Scientific) and Tape Station 4150 (Agilent Technologies). RNA-seq libraries were prepared using the NEBNext Ultra™ RNA Library Prep Kit (New England Biolabs) with the poly(A) mRNA magnetic isolation module (NEB #E7490). Briefly, after poly(A) enrichment of 0.8 ng of total RNA, mRNA was fragmented to ~100–200 nt, before synthesis of the first- and second cDNA strands. The resulting cDNA was purified, end-repaired, and used for adaptor ligation followed by barcoding using NEBNext Multiplex Oligos (New England Biolabs). PCR enrichment was done with 9 cycles, and the amplified libraries were purified using AMPure XP beads (Beckman Coulter, Inc.). In total, 14 libraries were prepared (4 for Control, 5 for SA8-UEL, and 5 for SA10-UEL groups). Libraries were quantified on the Tape Station 4150 (Agilent Technologies), pooled at equimolar ratios, and sequenced as paired-end reads (150 bp) on an Illumina NovaSeq 6000 sequencer (Illumina) at Novogene. The datasets generated in this study are available at the NCBI BioProject database under accession number PRJNA1049341.

2.6 Bioinformatic analysis

Adapter sequences and low-quality reads (quality < 20) were removed from the raw reads using *fastp* software (34) (version 0.23.2). Quality-trimmed reads were mapped to the Nile tilapia genome (accession number MKQE00000000.2) downloaded from NCBI (https://ftp.ncbi.nlm.nih.gov/), using HISAT2 (35) (version 2.2.1), and reads were annotated using *featureCounts* (36) (version 2.0.3). Differential expression of genes across treatment groups was analyzed using the R package limma (37), with the criteria |Log2 fold change| ≥ 1 and adjusted p-value of ≤ 0.05 (Benjamini–Hochberg multiple test correction method). Using the R pheatmap package, a heatmap was generated to visualize the fold change values of selected transcripts across different conditions. Genes were categorized into functional groups based on their biological roles, and comparisons with nonsignificant log2 fold change values were treated as zero. Row clustering was performed using hierarchical clustering with Euclidean distance and average linkage method. Enrichment of KEGG pathways and gene ontology (GO) was performed in g:Profiler (38) with a significance threshold of 0.05 (g:SCS multiple test correction method). The packages ggplot2 and GOplot in R were employed to visualize the data.

2.7 Fish challenge for biological validation

Following the same experimental setup from the first challenge, we conducted a new experiment to validate our initial transcriptomic findings. The strains of *S. agalactiae* were cultured in TSB (Acumedia) and incubated at 30°C for 18 hours. Subsequently, bacterial cells were collected by centrifugation at 10,000 × g for 20 minutes at 4°C. The bacterial pellets were washed twice with 0.85% saline solution, employing the same centrifugation parameters, and resuspended. The optical density (OD) from each suspension was measured at 620 nm using a spectrophotometer. The OD for the strain SA8-UEL was adjusted to 0.79 and for the SA10-UEL strain to 0.85, to achieve a final bacterial concentration of approximately 1×10^9 CFU/mL for each strain.

In this trial, fish from the challenged groups were intraperitoneally injected with 0.1 mL of the respective bacterial suspension (1×10^8 CFU/mL). This dosage is slightly higher than in the original experiment (see section 2.4) to increase the incidence of neurological symptoms to 25% of challenged animals. Fish from the control group were injected with an equal volume of sterile saline (0.85%). Fish exhibiting erratic swimming behavior were euthanized and 21 brain samples (7 from each group) were collected.

2.8 Gene expression analysis by qRT-PCR

The transcriptomic results and expression analysis of ten genes (Supplementary Table 2) were validated by qRT-PCR using samples obtained from the biological validation study. Primers for the selected genes were designed using the PrimerQuest™ tool from IDT (Integrated DNA Technologies) (https://eu.idtdna.com/PrimerQuest/). Primer secondary structures and dimers were

assessed with NetPrimer (Premier Biosoft). The primers for reference and target genes are given in Supplementary Table 2.

Briefly, 1 µg of total RNA extracted from each sample as mentioned previously, was reverse transcribed using the QuantiTect Reverse Transcription kit (Qiagen), according to the manufacturer's instructions. The obtained cDNA was diluted 50 times with nuclease-free water and used as a PCR template. The PCR reactions to validate the primers were carried out using the AmpliTaq Gold™ 360 Master Mix (Applied Biosystems™), on a C1000 Touch™ thermal cycler (Bio-Rad) programmed as follows: 95°C for 3 min, 40 cycles of 95°C for 30 s, 58-62°C for 34 s, and 72°C for 1 min, followed by another cycle of 72°C for 5 min. PCR products were analyzed by electrophoresis on a 1% (w/v) agarose gel, stained with SYBR Safe (Invitrogen™), and visualized in NuGenius Gel Documentation System (Syngene™) with the O'GeneRuler Express DNA Ladder 5 kb (Thermo Fisher Scientific). Water (negative control) and Nile tilapia DNA (positive control) were used as controls for the PCR reactions. After confirming the correct size of the amplicons, we carried out the qPCR.

The qPCR reactions were conducted using the SYBR Green qPCR Master Mix (Thermo Fisher Scientific) on a CFX96™ Real-Time PCR System (Bio-Rad) programmed as follows: 95°C for 3 min, 40 cycles of 95°C for 30 s, 58-62°C for 34 s, and 72°C for 1 min, followed by a melting curve analysis. The reactions were performed in duplicates of 7 biological replicates in each group. Data were acquired and analyzed using the CFX Maestro software (Bio-Rad).

Using geNorm (39) a geometric normalization factor was computed for each of the samples based on the relative quantities of the two most stable genes (tubulin alpha chain-like (*tuba*) and ubiquitin-conjugating enzyme (*ubce*)) among the set of four reference genes tested, which also included elongation factor 1-alpha (*eef1a*) and beta-2-microglobulin (*b2m*) (40). The relative expression levels were calculated relative to the normalization factors using the $2^{-\Delta\Delta Ct}$ method (41), taking the efficiency of each reaction into account.

For the correlation between RNA-Seq and qPCR data, the average Log2 fold change was calculated for each group within both datasets. These average fold changes were then compared between the infected groups (SA8-UEL and SA10-UEL) and the control group. The significance of differences between the RNA-Seq and qPCR data was analyzed using the Mann-Whitney U Test (Wilcoxon rank-sum test) ($p < 0.05$). All results are presented in Supplementary Figure 1 as mean ± standard error.

2.9 Detection of *S. agalactiae* in brain tissue by qPCR

To confirm bacterial presence within brain tissue, we performed qPCR targeting the *S. agalactiae rpoB* gene, which encodes the RNA polymerase beta subunit. The analysis utilized cDNA synthesized from samples obtained during the biological validation study. Amplification was carried out using the primers rpoB_F1 (5'-CACAATTCATGGACCAACACAAC-3') and rpoB_R1 (5'-GGCGTTTGTGCGACAATTCT-3') (42). The qPCR followed the same parameters as those used in the gene expression assays, with a 60°C annealing temperature.

3 Results

3.1 RNA sequencing analysis

A total of 306,649,706 raw reads were obtained from 14 libraries (4 from the Control group, 5 from the SA8-UEL strain exposed group, and 5 from the SA10-UEL strain exposed group), with a range of 15,272,516 to 26,377,837 per library. After adapter trimming and quality filtering, 303,492,279 reads were obtained and 277,440,575 reads were mapped to the reference genome, with an overall mapping rate of 91.3% (Table 1). Principal component analyses (PCA) revealed the differential clustering of the SA8-UEL, SA10-UEL, and Control groups across the first principal component (PC1), accounting for 35.4% of data variability (Figure 1).

3.2 Differential gene expression analysis

The analysis of global transcriptomic changes in the brain of Nile tilapia exposed to the SA8-UEL strain of *S. agalactiae* in comparison to the control group revealed 5,028 significantly differentially expressed genes (DEGs, |Log2 fold change| ≥ 1, Benjamini-Hochberg adjusted p-value ≤ 0.05) (3,281 upregulated and 1,747 downregulated), and a total of 997 DEGs in the SA10-UEL strain exposed group (965 upregulated and 32 downregulated). Also, 1,752 genes were differentially expressed (1,182 upregulated and 570 downregulated) between SA8-UEL and SA10-UEL exposed groups (Figures 2, 3, Supplementary Data Sheet 1).

Exposure to either *S. agalactiae* strain in Nile tilapia resulted in upregulation of immune and inflammation-related markers, including macrophage mannose receptor 1 (*MRC1*), *CD209* antigen, *granulin*, CXCL10, prostacyclin synthase, and interleukins *il-8*, *il-1β*, and il-4–induced 1 (IL4I1) (Figure 4, Table 2). Downregulation of genes involved in tissue repair (*beta-crystallin B1* and *B3*) and oxygen transport (hemoglobin subunit alpha-B and hemoglobin subunit beta-A) was also observed.

The comparison between Nile tilapia exposed to the SA8-UEL strain with those exposed to the SA10-UEL strain revealed distinct patterns in the expression of pathogen recognition-related genes. Specifically, *LOC102083301*, coding deleted in malignant brain tumors 1 protein and *pglypr5* were upregulated in response to SA8-UEL, while *LOC102079007*, coding C-type lectin domain family 4 member M-like was downregulated. Furthermore, inflammatory markers, such as L-amino-acid oxidase (LAAO), IL4I1, *ptgs2*, *tp53i3*, and *acod1*, were also upregulated.

Some genes involved in neuroplasticity were also differentially expressed between the two strains. Among these, the ones coding matrix metallopeptidases 13a, 9, and 19 were upregulated, while brain aromatase and pro-melanin-concentrating hormone (*pmch*) were downregulated in response to SA8-UEL compared to the SA10-UEL strain.

TABLE 1 Summary of assembly statistics for the transcripts obtained from *S. agalactiae* exposed (SA8-UEL or SA10-UEL strains) and control Nile tilapia brain.

Group	Sample ID	Raw read number	Clean read number	Total mapped (%)*
Control	TIL01008	18824055	18676959	90.7
Control	TIL01009	22353288	22231832	89.5
Control	TIL01010	23150678	23047138	89.0
Control	TIL01011	24891027	24466305	91.2
SA8-UEL	TIL01111	19522409	19010902	91.1
SA8-UEL	TIL01112	22260859	22056378	91.6
SA8-UEL	TIL01113	22170619	21834436	92.1
SA8-UEL	TIL01114	21524533	21380984	93.9
SA8-UEL	TIL01115	23498111	23358731	89.9
SA10-UEL	TIL01210	23641051	23502210	90.5
SA10-UEL	TIL01212	23281400	22945481	93.3
SA10-UEL	TIL01214	15272516	15089281	93.5
SA10-UEL	TIL01215	26377837	26130739	92.5
SA10-UEL	TIL01216	19881323	19760903	90.1

*Percentage of the reads mapped to the reference genome.

3.3 Gene ontology enrichment and pathways analysis

After sorting, 4,979 DEGs (39% of the total) were categorized into 499 functional groups of three major categories (molecular function, biological process, cellular component) and 40 pathways (Supplementary Data Sheet 2). No biological pathways were enriched in the analysis of downregulated DEGS in the SA10-UEL strain exposed groups.

The differentially upregulated genes in the exposed groups were enriched in terms associated with cytokine receptors interaction, lysosome, and pathogens infection, whereas genes downregulated in the exposed groups caused the significant enrichment of GO terms related to signaling and cell communication. When comparing tilapia exposed to the SA8-UEL versus SA10-UEL strains, DEGs connected to immune and signaling receptors such as cytokines, NOD-like, and Toll-like were upregulated, whereas DEGs involved in signaling and neuroactive receptors were downregulated (Figure 5). The list of annotated DEGs and associated GO terms and pathways in both strains (SA8-UEL and SA10-UEL) compared to the control group and between each other is presented in Supplementary Data Sheet 2.

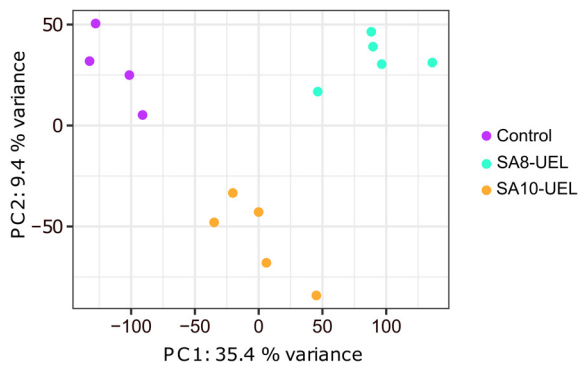

FIGURE 1
Principal component analysis plot shows the clear clustering of Control, SA8-UEL, and SA10-UEL groups.

3.4 Validation of RNA-Seq profiles by qPCR

To validate the DEGs identified by the RNA-Seq, ten genes with different expression patterns were selected for qPCR confirmation. The fold changes from qPCR were compared to those obtained by RNA-Seq. Among the ten genes examined, eight (*LOC100710283*, *LOC100706287*, *pglyrp5*, *granulin*, *LOC100700788*, *il-8*, *LOC100707066*, and *LOC100703315*) showed consistent expression trends across both methods (Supplementary Figure 1). Although there were statistically significant differences in the fold changes between RNA-Seq and qPCR for some genes, the overall expression trends within the infected groups were similar between the two techniques. Specifically, despite variations in the magnitude of fold changes, the direction of expression (upregulation) and the relative amplitude of changes between groups observed in RNA-Seq were consistent with those identified by qPCR.

3.5 Confirmation of *S. agalactiae* brain infection by qPCR

The qPCR results confirmed the presence of bacterial RNA in the brain of exposed fish (Supplementary Table 3). Amplification of

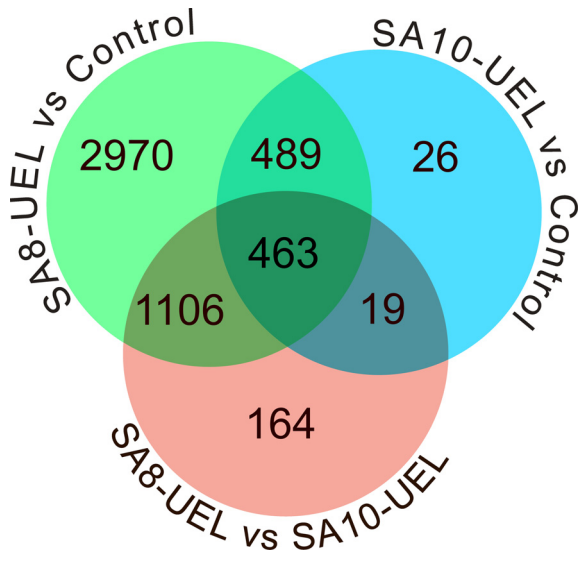

FIGURE 2
Venn diagram showing the distribution of differentially expressed genes among the comparisons between Control, SA8-UEL, and SA10-UEL groups.

rpoB transcripts was detected in the SA8-UEL (mean Cq value of 35.11 ± 1.28), and SA10-UEL (mean Cq value of 36.56 ± 1.66) challenged groups. No bacterial RNA was detected in the control group samples.

4 Discussion

The present transcriptomics study focused on investigating the molecular responses in the brain of Nile tilapia following intraperitoneal injection of two serotypes of *S. agalactiae*. While this challenge approach does not mimic the natural infection route (e.g., mucosal surfaces), it was selected to ensure consistent bacterial dose delivery and bypass potential variability associated with natural infection routes. Our qPCR and transcriptomic data suggest that *S. agalactiae* breached the BBB, damaging the CNS through acute inflammation. Comparative analysis between pathogen-exposed and control groups revealed significant upregulation of genes associated with immune response and inflammation, alongside downregulation of genes related to neuroendocrine regulation and tissue repair.

Following exposure to *S. agalactiae*, we observed increased expression of *rel*, *relb*, and *nfkb2*, indicating activation of the nuclear factor κB (NF-κB) signaling cascade. This pathway is important for immune regulation and is known to induce the expression of pro-inflammatory mediators (43). Notably, two of the most relevant downstream targets of NF-κB, *CXCL10* and *il-8*, were also upregulated. These chemokines are associated with immune cell recruitment to infection sites. *CXCL10* has chemotactic activity towards T cells, macrophages, and natural killer cells (44, 45), while *il-8* recruits neutrophils (46). Notably, *CXCL10* has also been implicated in increased BBB permeability, which could facilitate immune cell migration into the brain (47).

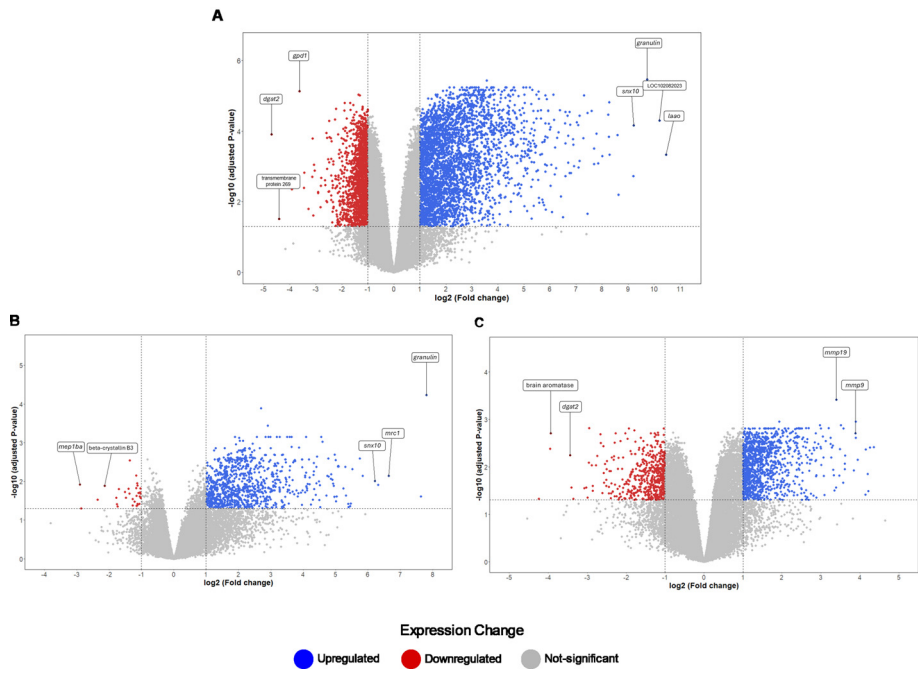

FIGURE 3
Distribution of DEGs based on fold changes for the Control, SA8-UEL, and SA10-UEL groups. **(A)** Volcano plot of DEGs identified between SA8-UEL exposed group and Control. **(B)** Volcano plot of DEGs identified between SA10-UEL exposed group and Control. **(C)** Volcano plot of DEGs identified between SA8-UEL exposed group and SA10-UEL exposed group. Genes represented in the plots correspond to specific LOC identifiers, including transmembrane protein 269 (LOC100689985), *laao* (LOC100703315), *mep1ba* (LOC100706112), beta-crystallin B3 (LOC100707280), and brain aromatase (LOC100534396). LOC102082023 is currently uncharacterized.

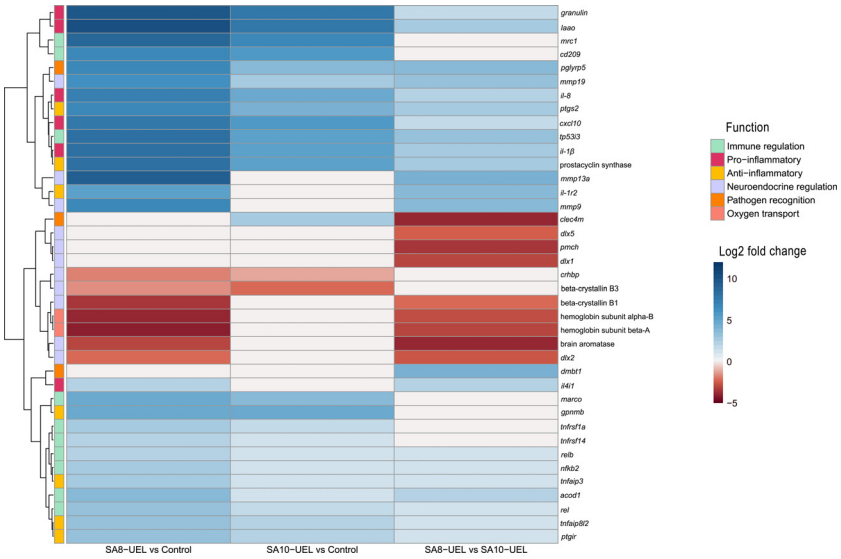

FIGURE 4
Heatmap of log2 fold change values for differentially expressed genes in Nile tilapia brains after infection with *Streptococcus agalactiae*. Rows represent genes, and columns represent pairwise comparisons between conditions (SA8-UEL vs Control, SA10-UEL vs Control, and SA8-UEL vs SA10-UEL). Colors indicate the magnitude and direction of fold change, with red shades indicating upregulation and blue shades indicating downregulation. Functional groups are annotated on the left. Comparisons with nonsignificant log2 fold change values were treated as 0. Genes represented in the plots correspond to specific LOC identifiers, including *laao* (LOC100703315), *mrc1* (LOC100710283), *cd209* (LOC1007062847), *cxcl10* (LOC100700788), *il1β* (LOC100707066), prostacyclin synthase (LOC100693506), *il1r2* (LOC100702124), beta-crystallin B1 (loc100707280), beta-crystallin B3 (LOC100705765), hemoglobin subunit alpha-B (LOC102080222), hemoglobin subunit beta-A (LOC100534396), dmbt1 (LOC102083301), and *il4i1* (LOC100697201).

In Mozambique tilapia, an alternatively spliced transcript of *granulin* modulates the expression of proinflammatory cytokines, including *il-1β* and *il-8* (48). In our study, the three genes—*granulin*, *il-1β*, and *il-8*—were upregulated, suggesting that *granulin* drives the expression of these cytokines. *il-1β* and *il-8* initiate innate immunity in vertebrates (49), mediate cellular communication, and trigger an inflammatory cascade (50).

The simultaneous upregulation of *il-1β*, *tnfrsf1a*, and *tnfrsf14* suggests BBB disruption, as *il-1β* is known to favor BBB plasticity and permeability, allowing immune cell infiltration into the CNS (51, 52). The *tnfrsf1a* and *tnfrsf14* genes encode receptors involved in tumor necrosis factor (TNF) signaling pathways (53). The expression of *tnfr1*, specifically, activates the NF-κB pathway (54), promoting inflammation and immune defense against pathogens (55, 56). TNF-α is a known contributor to BBB permeability and can lead to increased infiltration of immune cells into the CNS (57). Although TNF-α was not significantly upregulated, the expression of its receptors suggests that this factor may be active.

An existing hypothesis regarding *S. agalactiae* invasion into Nile tilapia's CNS suggests that immune cells may function as "Trojan horses", transporting the bacteria across the BBB (58). This idea is supported by the upregulated expression of macrophage mannose receptor 1 (*mrc1*), *CD209* antigen (DC-SIGN), and *marco* (coding for MARCO, macrophage receptor with collagenous structure). MRC1 and *CD209* are members of the C-type lectin superfamily, expressed in macrophages and dendritic cells (59, 60), while MARCO, a scavenger receptor, is expressed in certain macrophage subsets (61). Macrophages and dendritic cells, being phagocytic, can engulf *S. agalactiae* (62, 63), and inadvertently transport the bacteria into the CNS, contributing to pathogen dissemination.

The combined activation of the NF-κB pathway, TNF-related receptors, and recruitment of phagocytic cells, along with enrichment in cytokine-cytokine receptor interactions, indicates a pro-inflammatory response to *S. agalactiae* in the tilapia brain. While inflammation serves to contain the pathogen, prolonged activation can be harmful to the CNS. The upregulation of specific anti-inflammatory genes suggests compensatory mechanisms attempting to limit tissue damage during infection. One of the mechanisms involves the activation of *tnfaip3* and *tnfaip8l2*, encoding tumor necrosis factor-α-induced proteins 3 (A20) and 8-like 2 (TIPE2), respectively. Both are known as inhibitors of the NF-κB pathway (64, 65). Additionally, the activation of prostacyclin signaling, evidenced by *ptgs2*, *ptgir*, and *LOC100693506*, and the upregulation of *gpnmb* (glycoprotein nmb). PTGS2 (prostaglandin-endoperoxide synthase 2) has been shown to participate in the immune responses of common carp against *Aeromonas hydrophila* (66). The prostacyclin I2 receptor (*ptgir*) and prostacyclin synthase (*LOC100693506*) encode components important for anti-inflammatory effects, including vasodilation and prevention of platelet aggregation (67). Such as the PTG2, the glycoprotein nmb has an anti-inflammatory role and promotes disease resolution (68). Despite these regulatory mechanisms, the immune response remains skewed toward inflammation, as evidenced by the expression of multiple pro-inflammatory mediators.

The downregulation of *crhbp* (corticotropin-releasing hormone binding protein) implies a disruption in neuroendocrine regulation, specifically regarding stress. Crhbp modulates the availability of

10.3389/fimmu.2024.1528721

TABLE 2 Highly differentially expressed genes in Nile tilapia brain exposed to *S. agalactiae* strains SA8-UEL and SA10-UEL, with Log2 fold change (p-adj < 0.05) and corresponding standard deviation (SD).

Gene	Description	Log2 fold change (± SD)		
		SA8-UEL vs Control	SA10-UEL vs Control	SA8-UEL vs SA10-UEL
rel	v-rel avian reticuloendotheliosis viral oncogene homolog	3.09 (± 0.19)	1.82 (± 0.20)	1.26 (± 0.16)
relb	v-rel avian reticuloendotheliosis viral oncogene homolog B	2.15 (± 0.19)	1.08 (± 0.19)	1.07 (± 0.16)
nfkb2	nuclear factor of kappa light polypeptide gene enhancer in B-cells 2	2.83 (± 0.17)	1.41 (± 0.17)	1.43 (± 0.16)
LOC100700788	C-X-C motif chemokine 10	7.59 (± 0.41)	5.74 (± 0.41)	1.85 (± 0.16)
il-8	interleukin-8	7.08 (± 0.50)	4.90 (± 0.52)	2.18 (± 0.20)
granulin	progranulin	9.73 (± 0.28)	7.80 (± 0.28)	1.92 (± 0.17)
LOC100707066	interleukin-1β	8.01 (± 0.43)	5.40 (± 0.43)	2.62 (± 0.16)
tnfrsf1a	tumor necrosis factor receptor superfamily, member 1a	2.73 (± 0.27)	1.86 (± 0.28)	–
tnfrsf14	tumor necrosis factor receptor superfamily, member 14	2.43 (± 0.24)	1.46 (± 0.24)	–
LOC100710283	macrophage mannose receptor 1	8.59 (± 0.44)	6.64 (± 0.44)	–
LOC100706287	CD209 antigen	6.89 (± 0.46)	5.84 (± 0.46)	–
marco	macrophage receptor with collagenous structure	4.64 (± 0.28)	3.87 (± 0.28)	–
tnfaip3	tumor necrosis factor-α-induced proteins 3	2.54 (± 0.18)	1.12 (± 0.18)	1.41 (± 0.16)
tnfaip8l2	tumor necrosis factor-α-induced proteins 8-like 2	3.34 (± 0.23)	2.22 (± 0.24)	1.12 (± 0.16)
ptgs2	prostaglandin-endoperoxide synthase 2	6.88 (± 0.47)	4.30 (± 0.49)	2.59 (± 0.20)
ptgir	prostaglandin I2 receptor	3.47 (± 0.35)	2.19 (± 0.37)	1.28 (± 0.21)
LOC100693506	prostacyclin synthase	8.29 (± 0.57)	5.40 (± 0.59)	2.90 (± 0.21)
gpnmb	glycoprotein nmb	4.80 (± 0.33)	4.72 (± 0.33)	–
crhbp	corticotropin-releasing hormone binding protein	-1.81 (± 0.23)	-1.15 (± 0.21)	–
LOC100705765	beta-crystallin B1	-3.44 (± 0.45)	–	-2.24 (± 0.47)
LOC100707280	beta-crystallin B3	-1.46 (± 0.66)	-2.14 (± 0.69)	–
LOC102083301	deleted in malignant brain tumors 1 protein	–	–	4.21 (± 0.32)
pglyrp5	peptidoglycan recognition protein 5	6.76 (± 0.57)	3.95 (± 0.64)	3.95 (± 0.34)
LOC102079007	C-type lectin domain family 4 member M-like	–	2.57 (± 0.47)	-3.95 (± 0.52)
LOC100703315	L-amino-acid oxidase	10.46 (± 0.54)	7.64 (± 0.53)	2.83 (± 0.16)
LOC100697201	interleukin 4–induced 1	2.02 (± 0.44)	–	2.30 (± 0.42)
tp53i3	tumor protein p53 inducible protein 3	8.27 (± 0.35)	5.08 (± 0.35)	3.19 (± 0.16)
acod1	aconitate decarboxylase 1	3.64 (± 0.18)	1.26 (± 0.17)	2.38 (± 0.16)
LOC100702124	interleukin-1 receptor type 2	5.17 (± 0.37)	–	3.89 (± 0.27)
mmp13a	matrix metallopeptidase 13a	9.20 (± 0.59)	–	4.15 (± 0.23)
mmp9	matrix metallopeptidase 9	6.78 (± 0.25)	–	3.89 (± 0.16)
mmp19	matrix metallopeptidase 19	6.13 (± 0.37)	2.74 (± 0.39)	3.39 (± 0.20)
LOC100534396	brain aromatase	-3.07 (± 0.21)	–	-3.93 (± 0.21)
pmch	pro-melanin-concentrating hormone	–	–	-3.36 (± 0.27)
dlx1	distal-less homeobox 1	–	–	-3.00 (± 0.33)
dlx2	distal-less homeobox 2	-2.15 (± 0.45)	–	-2.57 (± 0.42)

(Continued)

TABLE 2 Continued

Gene	Description	Log2 fold change (± SD)		
		SA8-UEL vs Control	SA10-UEL vs Control	SA8-UEL vs SA10-UEL
dlx5	distal-less homeobox 5	–	–	-2.45 (± 0.37)
LOC102080222	hemoglobin subunit alpha-B	-3.91 (± 0.17)	–	-2.86 (± 0.16)
LOC100704059	hemoglobin subunit beta-A	-4.09 (± 0.17)	–	-3.03 (± 0.16)

corticotropin-releasing hormone (CRH), essential for stress and behavioral responses in fish, as part of the hypothalamic-pituitary-interrenal (HPI) axis (69). Similarly, the downregulation of beta-crystallin genes (*LOC100705765* and *LOC100707280*), involved in preserving the transparency and refractive index of the eye lens (70), may explain the corneal opacity visible in fish with streptococcosis.

Comparing the results between SA8-UEL and SA10-UEL strains-exposed animals, we observed divergent expressions in pathogen recognition-related genes. *LOC102083301*, encoding Deleted in malignant brain tumors 1 (Dmbt1) protein, and *pglyrp5*, a gene in the peptidoglycan recognition protein (PGRP) family, were upregulated in response to SA8-UEL. This result suggests the potential for each *S. agalactiae* strain to interact differently with the host's immune system, engaging different pathogen recognition pathways and consequently immune response initiation. In Nile tilapia, PGRP-SC, a member of the PGRP family, already demonstrated Zn^{2+}-dependent peptidoglycan-degrading activity against *S. agalactiae* (71). Similarly, the Dmbt1 protein was already found to be upregulated in cells in response to proinflammatory stimuli and interacting with streptococcal cell wall adhesins (72). This upregulation suggests an immune recognition response that facilitates bacterial cell wall degradation and inflammation in SA8-UEL-infected fish. In contrast, the downregulation of the gene that encodes Clec4m (C-type lectin domain family 4 member M-like) suggests a different recognition mechanism for the SA10-UEL strain. Previous studies on Mincle, another C-type lectin receptor, characterized its ability to recognize different serotypes of *Streptococcus pneumoniae*, but with a limited role in bacterial phagocytosis and cytokine production (73). This finding suggests that Clec4m may recognize SA10-UEL without directly promoting immune activation, possibly contributing to delayed pathogen clearance in SA10-UEL-exposed fish.

The faster immune activation in SA8-UEL-exposed fish, driven by Dmbt1 and PGRP5, seems to elicit a more intense response, as indicated by the upregulation of *tnfaip3*, *nfkb2*, and *il-8*, all components of the NF-κB signaling pathway. The activation of this pathway is associated with strong pro-inflammatory responses, typically associated with acute infection control (74, 75). Additional genes involved in inflammation, including L-amino-acid oxidase (LAAO), *LOC100697201* (IL4I1, Interleukin 4-induced 1), *tp53i3* (tumor protein p53 inducible protein 3), *acod1* (aconitate decarboxylase 1), *ptgs2* (prostaglandin-endoperoxide synthase 2), and *LOC100702124* (IL1R2, interleukin-1 receptor type 2) were also upregulated. LAAO and IL4I1 contribute to bacterial defense by producing hydrogen peroxide, a compound that has antibacterial and pro-inflammatory effects (76–78). The activation of immune response is indicated by upregulation of *tp53i3* and *acod1*. *tp53i3* is associated with cellular stress responses and DNA repair; with dual roles promoting DNA repair under moderate stress, or inducing apoptosis when damage is irreparable (79, 80). The expression of *acod1* has already been proven to be important in anti-bacterial immunity in fish macrophages following lipopolysaccharide (LPS)

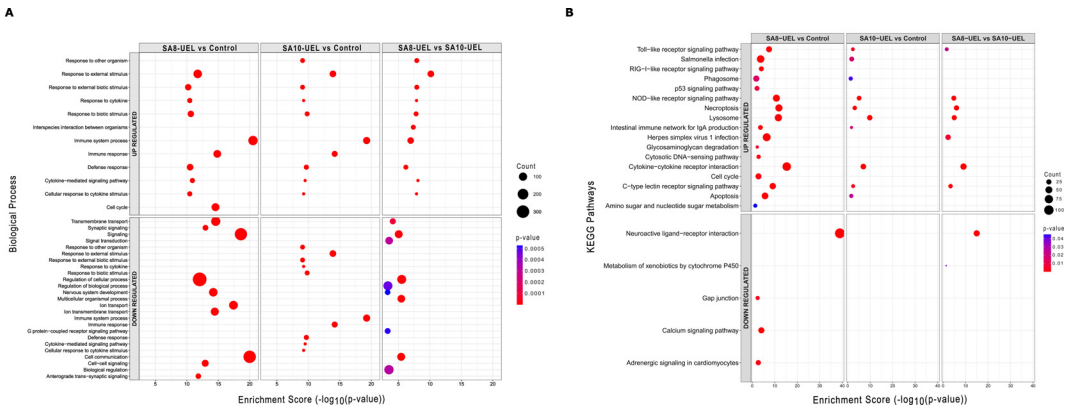

FIGURE 5
Gene Ontology (GO) biological processes and KEGG pathway enrichment analysis of differentially expressed genes in Nile tilapia brain following exposure to *Streptococcus agalactiae* strains SA8-UEL and SA10-UEL. The x-axis represents the enrichment score ($-\log_{10}$(p-value)), while the size of the circles represents the number of DEGs in each category, and colors indicate statistical significance (p-value). **(A)** Top 10 enriched GO biological processes for upregulated and downregulated DEGs. **(B)** KEGG pathway enrichment analysis for upregulated and downregulated DEGs.

stimulation (81–83). Moreover, the upregulation of *ptgs2* and IL1R2 shows a compensatory movement to counterbalance intense inflammation. IL1R2 is a decoy receptor and may help prevent excessive IL-1-driven signaling (84).

In response to SA8-UEL, metallopeptidases *mmp13a*, *mmp9*, and *mmp19*, which are involved in matrix remodeling and tissue repair, were also upregulated. In mammals, MMP-13 can activate MMP-9, recruiting immune cells and promoting wound healing (85, 86). MMP-19 may help regulate tissue integrity and limit damage by enhancing leukocyte infiltration, axonal regeneration, and astrogliosis for CNS recovery (87).

SA8-UEL exposure also appears to disrupt hormonal pathways in the Nile tilapia brain, as indicated by the downregulation of brain aromatase and *pmch* (pro-melanin concentrating hormone). Brain aromatase is involved in neurogenesis and neural repair (88, 89), while *PMCH* regulates appetite and behavior (90, 91). Reduced *pmch* expression correlates with the anorexigenic behavior observed in infected fish, suggesting that the SA8-UEL strain may intensify appetite suppression, likely as an adaptive response. Additionally, the downregulation of DLX genes family, particularly *dlx1*, *dlx2*, and *dlx5*. In zebrafish, the increased expression of *dlx* is associated with compensatory mechanisms for neuronal loss (92). The reduced expression of these genes in SA8-UEL-exposed fish may indicate more extensive tissue damage or a reduced regeneration capacity in comparison to SA10-UEL-exposed fish. Overall, SA8-UEL infection modulates genes that may lead to rapid immune activation, inflammation, and tissue repair. This shift is evident by the upregulation of genes involved in inflammation and tissue remodeling, along with the downregulation of genes involved in oxygen transport, neuroendocrine regulation, and behavioral responses. The faster immune response in SA8-UEL-exposed fish may explain the steady mortality rate, while the delayed response in SA10-UEL-exposed fish corresponds with acute mortality peaks within the initial days post-infection, and more severe CNS symptoms Furthermore, the SA10-UEL strain induced more pronounced neuroendocrine disruptions, likely contributing to the erratic behavior observed (Supplementary Figure 2).

During validation of the DEGs, 8 out of 10 genes analyzed showed consistent expression patterns across RNA-Seq and qPCR. Discrepancies in fold change were observed in two genes. *LOC102083301* was downregulated in the qPCR analysis and upregulated in the RNA-Seq results, and the *pmch* gene downregulated during RNA-Seq analysis and upregulated in qPCR in the SA8-UEL exposed group. These differences may be attributed to the use of samples from independent experiments or incorrect assignment of RNA-Seq reads to paralogous genes. Despite these minor inconsistencies, the qPCR validation supports the overall trends observed in the RNA-Seq data, indicating the reliability and accuracy of the differential expression analysis.

5 Conclusions

Our findings suggest that Nile tilapia exhibit distinct immune responses to *S. agalactiae* serotypes Ib and III, with serotype-specific gene expression profiles indicating differential interactions with the host's immune and neuroendocrine pathways. A graphical summary of the main findings of this manuscript is depicted in Figure 6.

Despite the intraperitoneal route of infection, our findings indicate that *S. agalactiae* breached the BBB, initiating CNS inflammation. We identified significant upregulation of immune-related genes, including important components of the NF-κB pathway, alongside the downregulation of genes associated with tissue repair and neuroendocrine functions.

In fish infected with the SA8-UEL strain (serotype Ib), the upregulation of *pglyrp5* and the gene that encodes Dmbt1, both

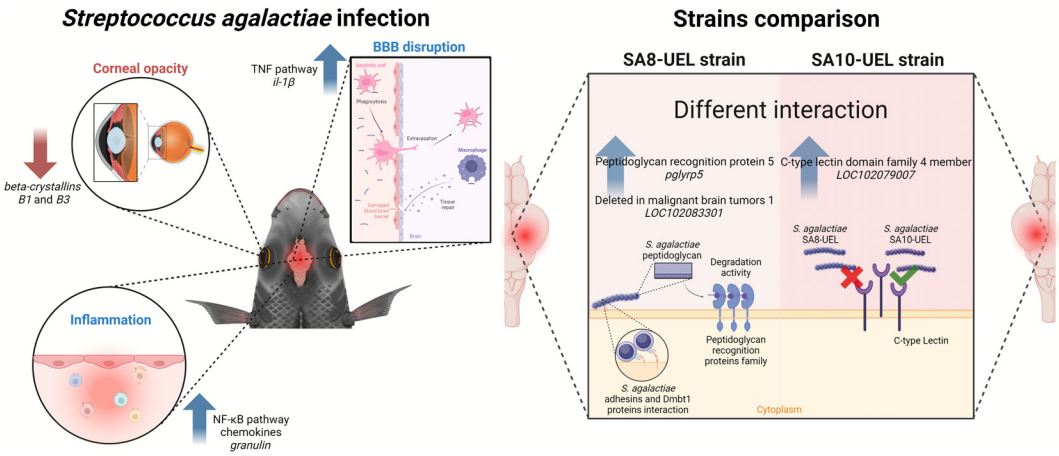

FIGURE 6
Overview of differential immune and physiological responses in Nile tilapia infected with two strains of *Streptococcus agalactiae* (SA8-UEL and SA10-UEL). Infection triggers inflammation, blood-brain barrier (BBB) disruption, and corneal opacity. BBB disruption permits immune cell infiltration into the brain, initiating tissue repair mechanisms but also allowing bacterial entry. Strain-specific host immune recognition responses are illustrated: SA8-UEL infection upregulates *pglyrp5* and *LOC102083301* (Deleted in Malignant Brain Tumors 1), promoting peptidoglycan degradation, while SA10-UEL infection upregulates *LOC102079007* (C-type lectin domain family 4 member), indicating distinct immune recognition pathways for each strain.

involved in bacterial cell wall recognition and degradation, indicates a more immediate immune response. In contrast, the SA10-UEL strain (serotype III) elicits a less pronounced immune activation, with the upregulation of the gene coding Clec4m. This C-type lectin receptor, although involved in bacterial recognition, does not directly trigger an immune response, potentially leading to insufficient pathogen clearance compared to serotype Ib. This differential response may explain the more severe CNS symptoms and behavioral disturbances, such as erratic swimming, observed in SA10-UEL-infected fish.

To the best of our knowledge, this is the first transcriptomic study to identify serotype-specific immune responses induced by two *S. agalactiae* strains in Nile tilapia. Understanding the immunological and neuroendocrine pathways activated by different bacterial serotypes provides important insights into host-pathogen interactions and can guide more targeted disease management strategies for the aquaculture industry.

Data availability statement

The datasets presented in this study can be found in online repositories. The names of the repository/repositories and accession number(s) can be found below: https://www.ncbi.nlm.nih.gov/, PRJNA1049341.

Ethics statement

The animal study was approved by Animal Ethics Committee of State University of Londrina, Brazil (process n&z.ousco; CEUA 45/2017). The study was conducted in accordance with the local legislation and institutional requirements.

Author contributions

RA: Conceptualization, Data curation, Formal analysis, Investigation, Methodology, Validation, Visualization, Writing – original draft, Writing – review & editing. KS: Methodology, Validation, Writing – review & editing. IK: Data curation, Formal Analysis, Supervision, Writing – review & editing. MM: Funding acquisition, Writing – review & editing. RJ: Funding acquisition, Writing – review & editing. LP-G: Conceptualization, Funding acquisition, Investigation, Methodology, Resources, Supervision, Writing – review & editing. LV: Conceptualization, Funding acquisition, Investigation, Methodology, Resources, Supervision, Writing – review & editing. JF: Conceptualization, Funding acquisition, Investigation, Methodology, Resources, Supervision, Writing – review & editing.

Funding

The author(s) declare financial support was received for the research, authorship, and/or publication of this article. This work was funded by the NORBRAQUA project (Research Council of Norway, grant nr. 310103) with additional support from the Coordenação de Aperfeiçoamento de Pessoal de Nível Superior (Brazil), Nord University (Norway) and the grant 'Severo Ochoa Centre of Excellence' accreditation (CEX2019-000928-S) funded by Agencia Estatal de Investigación 10.13039/501100011033 (Spain).

Conflict of interest

RJ was employed by GenoMar Genetics AS.

The remaining authors declare that the research was conducted in the absence of any commercial or financial relationships that could be construed as a potential conflict of interest.

Generative AI statement

The author(s) declare that no Generative AI was used in the creation of this manuscript.

Publisher's note

Supplementary material

The Supplementary Material for this article can be found online at: https://www.frontiersin.org/articles/10.3389/fimmu.2024.1528721/full#supplementary-material

References

1. Moreno-Andrés J, Rueda-Márquez JJ, Homola T, Vielma J, Moríñigo MÁ, Mikola A, et al. A comparison of photolytic, photochemical and photocatalytic processes for disinfection of recirculation aquaculture systems (RAS) streams. *Water Res.* (2020) 181:115928. doi: 10.1016/j.watres.2020.115928

2. Maulu S, Hasimuna OJ, Mphande J, Munang'andu HM. Prevention and control of Streptococcosis in tilapia culture: A systematic review. *J Aquat Anim Health.* (2021) 33:162–77. doi: 10.1002/aah.10132

3. FAO. *The State of World Fisheries and Aquaculture 2022.* Rome, Italy: FAO (2022). doi: 10.4060/cc0461en

4. Phuoc NN, Linh NTH, Crestani C, Zadoks RN. Effect of strain and enviromental conditions on the virulence of *Streptococcus agalactiae* (Group B Streptococcus; GBS) in red tilapia (*Oreochromis* sp.). *Aquaculture.* (2021) 534:736256. doi: 10.1016/j.aquaculture.2020.736256

5. Haenen OLM, Dong HT, Hoai TD, Crumlish M, Karunasagar I, Barkham T, et al. Bacterial diseases of tilapia, their zoonotic potential and risk of antimicrobial resistance. *Rev Aquac*. (2023) 15:154–85. doi: 10.1111/raq.12743

6. Musa N, Wei LS, Musa N, Hamdan RH, Leong LK, Wee W, et al. Streptococcosis in red hybrid tilapia (*Oreochromis niloticus*) commercial farms in Malaysia. *Aquac Res*. (2009) 40:630–2. doi: 10.1111/j.1365-2109.2008.02142.x

7. Abu-Elala NM, Abd-Elsalam RM, Younis NA. Streptococcosis, Lactococcosis and Enterococcosis are potential threats facing cultured Nile tilapia (*Oreochomis niloticus*) production. *Aquac Res*. (2020) 51:4183–95. doi: 10.1111/are.14760

8. Gallage S, Katagiri T, Endo M, Maita M. Comprehensive evaluation of immunomodulation by moderate hypoxia in S. agalactiae vaccinated Nile tilapia. *Fish Shellfish Immunol*. (2017) 66:445–54. doi: 10.1016/j.fsi.2017.05.041

9. Laith AA, Abdullah MA, Nurhafizah WWI, Hussein HA, Aya J, Effendy AWM, et al. Efficacy of live attenuated vaccine derived from the *Streptococcus agalactiae* on the immune responses of *Oreochromis niloticus*. *Fish Shellfish Immunol*. (2019) 90:235–43. doi: 10.1016/j.fsi.2019.04.052

10. Amal MNA, Zamri-Saad M. Streptococcosis in tilapia (*Oreochromis niloticus*): A Review. *Pertanika J Trop Agric Sci*. (2011) 34:195–206.

11. Buller NB. *Bacteria from Fish and Other Aquatic Animals: A Practical Identification Manual*. Cambridge: CABI Publishing (2004).

12. Joshi R, Skaaurd A, Tola Alvarez A. Experimental validation of genetic selection for resistance against *Streptococcus agalactiae* via different routes of infection in the commercial Nile tilapia breeding programme. *J Anim Breed Genet*. (2021) 138:338–48. doi: 10.1111/jbg.12516

13. Deng L, Li Y, Geng Y, Zheng L, Rehman T, Zhao R, et al. Molecular serotyping and antimicrobial susceptibility of *Streptococcus agalactiae* isolated from fish in China. *Aquaculture*. (2019) 510:84–9. doi: 10.1016/j.aquaculture.2019.05.046

14. Leal CAG, Silva BA, Colombo SA. Susceptibility profile and epidemiological cut-off values are influenced by serotype in fish pathogenic *Streptococcus agalactiae*. *Antibiotics*. (2023) 12:1513. doi: 10.3390/antibiotics12121726

15. Sapugahawatte DN, Li C, Dharmaratne P, Zhu C, Yeoh YK, Yang J, et al. Prevalence and characteristics of *Streptococcus agalactiae* from freshwater fish and pork in Hong Kong wet markets. *Antibiotics*. (2022) 11:30397. doi: 10.3390/antibiotics11030397

16. Zhang D, Liu Z, Ren Y, Wang Y, Pan H, Liang D, et al. Epidemiological characteristics of *Streptococcus agalactiae* in tilapia in China from 2006 to 2020. *Aquaculture*. (2022) 549:737724. doi: 10.1016/j.aquaculture.2021.737724

17. Slotved HC, Kong F, Lambertsen L, Sauer S, Gilbert GL. Serotype IX, a proposed new *Streptococcus agalactiae* serotype. *J Clin Microbiol*. (2007) 45:2929–36. doi: 10.1128/JCM.00117-07

18. Chideroli RT, Amoroso N, Mainardi RM, Suphoronski SA, de Padua SB, Alfieri AF, et al. Emergence of a new multidrug-resistant and highly virulent serotype of *Streptococcus agalactiae* in fish farms from Brazil. *Aquaculture*. (2017) 479:45–51. doi: 10.1016/j.aquaculture.2017.05.013

19. Kayansamruaj P, Pirarat N, Hirono I, Rodkhum C. Increasing of temperature induces pathogenicity of *Streptococcus agalactiae* and the up-regulation of inflammatory related genes in infected Nile tilapia (*Oreochromis niloticus*). *Vet Microbiol*. (2014) 172:265–71. doi: 10.1016/j.vetmic.2014.04.013

20. Ndong D, Chen YY, Lin YH, Vaseeharan B, Chen JC. The immune response of tilapia *Oreochromis mossambicus* and its susceptibility to *Streptococcus iniae* under stress in low and high temperatures. *Fish Shellfish Immunol*. (2007) 22:686–94. doi: 10.1016/j.fsi.2006.08.015

21. Qiang J, Yang H, Wang H, Kpundeh MD, Xu P. Interacting effects of water temperature and dietary protein level on hematological parameters in Nile tilapia juveniles, *Oreochromis niloticus* (L.) and mortality under *Streptococcus iniae* infection. *Fish Shellfish Immunol*. (2013) 34:8–16. doi: 10.1016/j.fsi.2012.09.003

22. Acar U, Kesbiç OS, Yilmaz S, Gültepe N, Türker A. Evaluation of the effects of essential oil extracted from sweet orange peel (*Citrus sinensis*) on growth rate of tilapia (*Oreochromis mossambicus*) and possible disease resistance against *Streptococcus iniae*. *Aquaculture*. (2015) 437:282–6. doi: 10.1016/j.aquaculture.2014.12.015

23. Guo JJ, Kuo CM, Chuang YC, Hong JW, Chou RL, Chen TI. The effects of garlic-supplemented diets on antibacterial activity against *Streptococcus iniae* and on growth in orange-spotted grouper, Epinephelus coioides. *Aquaculture*. (2012) 364–365:33–8. doi: 10.1016/j.aquaculture.2012.07.023

24. Wu YR, Gong QF, Fang H, Liang WW, Chen M, He RJ. Effect of *Sophora flavescens* on non-specific immune response of tilapia (GIFT *Oreochromis niloticus*) and disease resistance against *Streptococcus agalactiae*. *Fish Shellfish Immunol*. (2013) 34:220–7. doi: 10.1016/j.fsi.2012.10.020

25. Yeh SP, Chang CA, Chang CY, Liu CH, Cheng W. Dietary sodium alginate administration affects fingerling growth and resistance to *Streptococcus* sp. and iridovirus, and juvenile non-specific immune responses of the orange-spotted grouper, *Epinephelus coioides*. *Fish Shellfish Immunol*. (2008) 25:19–27. doi: 10.1016/j.fsi.2007.11.011

26. Wang B, Gan Z, Cai S, Wang Z, Yu D, Lin Z, et al. Comprehensive identification and profiling of Nile tilapia (*Oreochromis niloticus*) microRNAs response to *Streptococcus agalactiae* infection through high-throughput sequencing. *Fish Shellfish Immunol*. (2016) 54:93–106. doi: 10.1016/j.fsi.2016.03.159

27. Zhang R, Zhang LL, Ye X, Tian YY, Sun CF, Lu MX, et al. Transcriptome profiling and digital gene expression analysis of Nile tilapia (*Oreochromis niloticus*) infected by *Streptococcus agalactiae*. *Mol Biol Rep*. (2013) 40:5657–68. doi: 10.1007/s11033-013-2667-3

28. Zhu J, Fu Q, Ao Q, Tan Y, Luo Y, Jiang H, et al. Transcriptomic profiling analysis of tilapia (*Oreochromis niloticus*) following *Streptococcus agalactiae* challenge. *Fish Shellfish Immunol*. (2017) 62:202–12. doi: 10.1016/j.fsi.2017.01.023

29. Zhu J, Li C, Ao Q, Tan Y, Luo Y, Guo Y, et al. Transcriptomic profiling revealed the signatures of acute immune response in tilapia (*Oreochromis niloticus*) following *Streptococcus iniae* challenge. *Fish Shellfish Immunol*. (2015) 46:346e353–353. doi: 10.1016/j.fsi.2015.06.027

30. Li H, Sun Y, Sun L. A teleost CXCL10 is both an immunoregulator and an antimicrobial. *Front Immunol*. (2022) 13:917697. doi: 10.3389/fimmu.2022.917697

31. Neely MN, Pfeifer JD, Caparon M. *Streptococcus*-zebrafish model of bacterial pathogenesis. *Infect Immun*. (2002) 70:3904–14. doi: 10.1128/IAI.70.7.3904-3914.2002

32. Zlotkin A, Chilmonczyk S, Eyngor M, Hurvitz A, Ghittino C, Eldar A. Trojan horse effect: Phagocyte-mediated *Streptococcus iniae* infection of fish. *Infect Immun*. (2003) 71:2318–25. doi: 10.1128/IAI.71.5.2318-2325.2003

33. Miles AA, Misra SS, Irwin JO. The estimation of the bactericidal power of the blood. *Epidemiol Infect*. (1938) 38:732–49. doi: 10.1017/S002217240001158X

34. Chen S, Zhou Y, Chen Y, Gu J. Fastp: An ultra-fast all-in-one FASTQ preprocessor. *Bioinformatics*. (2018) 34:i884–90. doi: 10.1093/bioinformatics/bty560

35. Kim D, Langmead B, Salzberg SL. HISAT: A fast spliced aligner with low memory requirements. *Nat Methods*. (2015) 12:357–60. doi: 10.1038/nmeth.3317

36. Liao Y, Smyth GK, Shi W. FeatureCounts: An efficient general purpose program for assigning sequence reads to genomic features. *Bioinformatics*. (2014) 30:923–30. doi: 10.1093/bioinformatics/btt656

37. Ritchie ME, Phipson B, Wu D, Hu Y, Law CW, Shi W, et al. Limma powers differential expression analyses for RNA-sequencing and microarray studies. *Nucleic Acids Res*. (2015) 43:e47. doi: 10.1093/nar/gkv007

38. Raudvere U, Kolberg L, Kuzmin I, Arak T, Adler P, Peterson H, et al. G:Profiler: A web server for functional enrichment analysis and conversions of gene lists (2019 update). *Nucleic Acids Res*. (2019) 47:W191–8. doi: 10.1093/nar/gkz369

39. Vandesompele J, De Preter K, Pattyn F, Poppe B, Van Roy N, De Paepe A, et al. Accurate normalization of real-time quantitative RT-PCR data by geometric averaging of multiple internal control genes. *Genome Biol*. (2002) 3:research0034. doi: 10.1186/gb-2002-3-7-research0034

40. Yang CG, Wang XL, Tian J, Liu W, Wu F, Jiang M, et al. Evaluation of reference genes for quantitative real-time RT-PCR analysis of gene expression in Nile tilapia (*Oreochromis niloticus*). *Gene*. (2013) 527:183–92. doi: 10.1016/j.gene.2013.06.013

41. Pfaffl MW. A new mathematical model for relative quantification in real-time RT-PCR. *Nucleic Acids Res*. (2001) 29:e45. doi: 10.1093/nar/29.9.e45

42. Florindo C, Ferreira R, Borges V, Spellerberg B, Gomes JP, Borrego MJ. Selection of reference genes for real-time expression studies in *Streptococcus agalactiae*. *J Microbiol Methods*. (2012) 90:220–7. doi: 10.1016/j.mimet.2012.05.011

43. Sun SC. The non-canonical NF-κB pathway in immunity and inflammation. *Nat Rev Immunol*. (2017) 17:545–58. doi: 10.1038/nri.2017.52

44. Lande R, Giacomini E, Grassi T, Remoli ME, Iona E, Miettinen M, et al. IFN-αβ released by *Mycobacterium tuberculosis*-infected human dendritic cells induces the expression of CXCL10: Selective recruitment of NK and activated T cells. *J Immunol*. (2003) 170:1174–82. doi: 10.4049/jimmunol.170.3.1174

45. Agostini C, Calabrese F, Rea F, Facco M, Tosoni A, Loy M, et al. CXCR3 and its ligand CXCL10 are expressed by inflammatory cells infiltrating lung allografts and mediate chemotaxis of T cells at sites of rejection. *Am J Pathol*. (2001) 158:1703–11. doi: 10.1016/S0002-9440(10)64126-0

46. Matsushima K, Yang D, Oppenheim JJ. Interleukin-8: An evolving chemokine. *Cytokine*. (2022) 153:155828. doi: 10.1016/j.cyto.2022.155828

47. Chai Q, She R, Huang Y, Fu ZF. Expression of neuronal CXCL10 induced by rabies virus infection initiates infiltration of inflammatory cells, production of chemokines and cytokines, and enhancement of blood-brain barrier permeability. *J Virol*. (2015) 89:870–6. doi: 10.1128/jvi.02154-14

48. Wu SH, Lin HJ, Lin WF, Wu JL, Gong HY. A potent tilapia secreted granulin peptide enhances the survival of transgenic zebrafish infected by *Vibrio vulnificus* via modulation of innate immunity. *Fish Shellfish Immunol*. (2018) 75:74–90. doi: 10.1016/j.fsi.2018.01.044

49. Dinarello CA. Proinflammatory cytokines. *Chest*. (2000) 118:503–8. doi: 10.1378/chest.118.2.503

50. Huising MO, Stet RJM, Savelkoul HFJ, Verburg-Van Kemenade BML. The molecular evolution of the interleukin-1 family of cytokines; IL-18 in teleost fish. *Dev Comp Immunol*. (2004) 28:395–413. doi: 10.1016/j.dci.2003.09.005

51. Tadesse Argaw A, Zhang Y, Snyder BJ, Zhao ML, Kopp N, Lee SC, et al. IL-1 regulates blood-brain barrier permeability via reactivation of the hypoxia-angiogenesis program. *J Immunol*. (2006) 177:5574–84. doi: 10.4049/jimmunol.177.8.5574

52. Blamire AM, Anthony DC, Rajagopalan B, Sibson NR, Perry VH, Styles P. Interleukin-1-induced changes in blood-brain barrier permeability, apparent diffusion coefficient, and cerebral blood volume in the rat brain: A magnetic resonance study. *J Neurosci*. (2000) 21:8153–9. doi: 10.1523/JNEUROSCI.20-21-08153.2000

53. Jang DI, Lee AH, Shin HY, Song HR, Park JH, Kang TB, et al. The role of tumor necrosis factor alpha (TNF-α) in autoimmune disease and current TNF-α inhibitors in therapeutics. *Int J Mol Sci*. (2021) 22:2719. doi: 10.3390/ijms22052719

54. Haas TL, Emmerich CH, Gerlach B, Schmukle AC, Cordier SM, Rieser E, et al. Recruitment of the linear ubiquitin chain assembly complex stabilizes the TNF-R1 signaling complex and is required for TNF-mediated gene induction. *Mol Cell*. (2009) 36:831–44. doi: 10.1016/j.molcel.2009.10.013

55. Aggarwal BB, Gupta SC, Kim JH. Historical perspectives on tumor necrosis factor and its superfamily: 25 years later, a golden journey. *Blood*. (2012) 119:651–65. doi: 10.1182/blood-2011-04-325225

56. Brenner D, Blaser H, Mak TW. Regulation of tumour necrosis factor signalling: Live or let die. *Nat Rev Immunol*. (2015) 15:362–74. doi: 10.1038/nri3834

57. Tsao N, Hsu HP, Wu CM, Liu CC, Lei HY. Tumour necrosis factor-alpha causes an increase in blood-brain barrier permeability during sepsis. *J Med Microbiol*. (2001) 50:812–21. doi: 10.1099/0022-1317-50-9-812

58. Cao J, Liu Z, Zhang D, Guo F, Gao F, Wang M, et al. Distribution and localization of *Streptococcus agalactiae* in different tissues of artificially infected tilapia (*Oreochromis niloticus*). *Aquaculture*. (2022) 546:737370. doi: 10.1016/j.aquaculture.2021.737370

59. Gazi U, Martinez-Pomares L. Influence of the mannose receptor in host immune responses. *Immunobiology*. (2009) 214:554–61. doi: 10.1016/j.imbio.2008.11.004

60. Mnich ME, van Dalen R, van Sorge NM. C-type lectin receptors in host defense against bacterial pathogens. *Front Cell Infect Microbiol*. (2020) 10:309. doi: 10.3389/fcimb.2020.00309

61. Kraal G, van der Laana LW, Elomaa O, Tryggvason K. The macrophage receptor MARCO. *Microbes Infect*. (2000) 2:313–6. doi: 10.1016/S1286-4579(00)00296-3

62. Jiang S, Sun L. Tongue sole CD209: A pattern-recognition receptor that binds a broad range of microbes and promotes phagocytosis. *Int J Mol Sci*. (2017) 18:1848. doi: 10.3390/ijms18091848

63. Yin X, Bai H, Mu L, Chen N, Qi W, Huang Y, et al. Expression and functional characterization of the mannose receptor (MR) from Nile tilapia (*Oreochromis niloticus*) in response to bacterial infection. *Dev Comp Immunol*. (2022) 126:104257. doi: 10.1016/j.dci.2021.104257

64. Zhang YH, Yan HQ, Wang F, Wang YY, Jiang YN, Wang YN, et al. TIPE2 inhibits TNF-α-induced hepatocellular carcinoma cell metastasis via Erk1/2 downregulation and NF-κB activation. *Int J Oncol*. (2015) 46:254–64. doi: 10.3892/ijo.2014.2725

65. Rossi MN, Federici S, Uva A, Passarelli C, Celani C, Caiello I, et al. Identification of a novel mutation in TNFAIP3 in a family with poly-autoimmunity. *Front Immunol*. (2022) 13:804401. doi: 10.3389/fimmu.2022.804401

66. Gao F, Shi X, Zhao Y, Qiao D, Pei C, Li C, et al. The role of CcPTGS2a in immune response against *Aeromonas hydrophila* infection in common carp (*Cyprinus carpio*). *Fish Shellfish Immunol*. (2023) 141:109058. doi: 10.1016/j.fsi.2023.109058

67. Cebola I, Peinado M. PTGIS (prostaglandin I2 (prostacyclin) synthase). *Atlas Genet Cytogenet Oncol Haematol*. (2011) 14(4):418–20. doi: 10.4267/2042/44740

68. Saade M, Araujo de Souza G, Scavone C, Kinoshita PF. The role of GPNMB in inflammation. *Front Immunol*. (2021) 12:674739. doi: 10.3389/fimmu.2021.674739

69. Kim JS, Han SY, Iremonger KJ. Stress experience and hormone feedback tune distinct components of hypothalamic CRH neuron activity. *Nat Commun*. (2019) 10:13639. doi: 10.1038/s41467-019-13639-8

70. Cvekl A, McGreal R, Liu W. Lens development and crystallin gene expression. *Prog Mol Biol Transl Sci*. (2015) 134:129–67. doi: 10.1016/bs.pmbts.2015.05.001

71. Gan Z, Chen S, Hou J, Huo H, Zhang X, Ruan B, et al. Molecular and functional characterization of peptidoglycan-recognition protein SC2 (PGRP-SC2) from Nile tilapia (*Oreochromis niloticus*) involved in the immune response to *Streptococcus agalactiae*. *Fish Shellfish Immunol*. (2016) 54:1–10. doi: 10.1016/j.fsi.2016.03.158

72. Rosenstiel P, Sina C, End C, Renner M, Lyer S, Till A, et al. Regulation of DMBT1 via NOD2 and TLR4 in intestinal epithelial cells modulates bacterial recognition and invasion. *J Immunol*. (2007) 178:8203–11. doi: 10.4049/jimmunol.178.12.8203

73. Rabes A, Zimmermann S, Reppe K, Lang R, Seeberger PH, Suttorp N, et al. The C-type lectin receptor mincle binds to *Streptococcus pneumoniae* but plays a limited role in the anti-pneumococcal innate immune response. *PloS One*. (2015) 10:e0117022. doi: 10.1371/journal.pone.0117022

74. Charlie-Silva I, Klein A, Gomes JMM, Prado EJR, Moraes AC, Eto SF, et al. Acute-phase proteins during inflammatory reaction by bacterial infection: Fish-model. *Sci Rep*. (2019) 9:41312. doi: 10.1038/s41598-019-41312-z

75. Bayne CJ, Gerwick L. The acute phase response and innate immunity of fish. *Dev Comp Immunol*. (2001) 25:725–43. doi: 10.1016/s0145-305x(01)00033-7

76. Rhee SG. Redox signaling: hydrogen peroxide as intracellular messenger. *Exp Mol Med*. (1999) 31:53–9. doi: 10.1038/emm.1999.9

77. Huang Y, Han X, Peng H, Wang X, Li R. Analysis of inhibition mechanisms of *Streptococcus agalactiae* by *Siganus oramin* L-amino acid oxidase. *Aquac Res*. (2022) 53:6205–18. doi: 10.1111/are.16093

78. Puiffe ML, Lachaise I, Molinier-Frenkel V, Castellano F. Antibacterial properties of the mammalian L-amino acid oxidase IL4I1. *PloS One*. (2013) 8:e54589. doi: 10.1371/journal.pone.0054589

79. Kotsinas A, Aggarwal V, Tan EJ, Levy B, Gorgoulis VG. PIG3: A novel link between oxidative stress and DNA damage response in cancer. *Cancer Lett*. (2012) 327:97–102. doi: 10.1016/j.canlet.2011.12.009

80. Lane D, Levine A. p53 research: the past thirty years and the next thirty years. *Cold Spring Harb Perspect Biol*. (2010) 2:a000893. doi: 10.1101/cshperspect.a000893

81. Wu R, Chen F, Wang N, Tang D, Kang R. ACOD1 in immunometabolism and disease. *Cell Mol Immunol*. (2020) 17:822–33. doi: 10.1038/s41423-020-0489-5

82. Li S, Cao Y, Cui X, Sun J. Aconitate decarboxylase 1 (Acod1) suppresses inflammatory stimuli-induced immune responses in Japanese flounder (*Paralichthys olivaceus*). *Aquaculture*. (2024) 593:741281. doi: 10.1016/j.aquaculture.2024.741281

83. Lee NT, Jenkins CG, Gilbert NG, Copeland NA. Cloning and analysis of gene regulation of a novel LPS-inducible cDNA. *Immunogenetics*. (1995) 41:263–70. doi: 10.1007/BF00172150

84. Peters VA, Joesting JJ, Freund GG. IL-1 receptor 2 (IL-1R2) and its role in immune regulation. *Brain Behav Immun*. (2013) 32:1–8. doi: 10.1016/j.bbi.2012.11.006

85. Chi H, Dong Z, Gan Q, Tang X, Xing J, Sheng X, et al. Matrix metalloproteinase 9 modulates immune response along with the formation of extracellular traps in flounder (*Paralichthys olivaceus*). *Fish Shellfish Immunol*. (2023) 133:108570. doi: 10.1016/j.fsi.2023.108570

86. Lemmens K, Bollaerts I, Bhumika S, de Groef L, Van Houcke J, Darras VM, et al. Matrix metalloproteinases as promising regulators of axonal regrowth in the injured adult zebrafish retinotectal system. *J Comp Neurol*. (2016) 524:1472–93. doi: 10.1002/cne.23920

87. Van Horssen J, Vos CMP, Admiraal L, Van Haastert ES, Montagne L, van der Valk P, et al. Matrix metalloproteinase-19 is highly expressed in active multiple sclerosis lesions. *Neuropathol Appl Neurobiol*. (2006) 32:585–93. doi: 10.1111/j.1365-2990.2006.00766.x

88. Garcia-Segura LM, Veiga S, Sierra A, Melcangi RC, Azcoitia I. Aromatase: A neuroprotective enzyme. *Prog Neurobiol*. (2003) 71:31–41. doi: 10.1016/j.pneurobio.2003.09.005

89. Garcia-Segura LM. Aromatase in the brain: Not just for reproduction anymore. *J Neuroendocrinol*. (2008) 20:705–12. doi: 10.1111/j.1365-2826.2008.01713.x

90. Matsuda K, Shimakura SI, Miura T, Maruyama K, Uchiyama M, Kawauchi H, et al. Feeding-induced changes of melanin-concentrating hormone (MCH)-like immunoreactivity in goldfish brain. *Cell Tissue Res*. (2007) 328:375–82. doi: 10.1007/s00441-006-0347-5

91. Matsuda K, Shimakura SI, Maruyama K, Miura T, Uchiyama M, Kawauchi H, et al. Central administration of melanin-concentrating hormone (MCH) suppresses food intake, but not locomotor activity, in the goldfish, *Carassius auratus*. *Neurosci Lett*. (2006) 399:259–63. doi: 10.1016/j.neulet.2006.02.005

92. Mendes HW, Taktek M, Duret T, Ekker M. Expression of *dlx* genes in the normal and regenerating brain of adult zebrafish. *PLoS One*. (2020) 15:e0229549. doi: 10.1371/journal.pone.0229549